Durable and Electrified Pavement for Dynamic Wireless Charging of Electric Vehicles

FINAL REPORT
August, 2022

Submitted by:

Hao Wang
Associate Professor

Lukai Guo
Postdoctoral Associate

Department of Civil and Environmental Engineering,
Rutgers, The State University of New Jersey
Piscataway, NJ 08854

External Project Manager

Edward Liu, Traffic Engineer, New Jersey Department of Transportation

David J. Goldberg Transportation Complex
1035 Parkway Avenue Trenton, NJ 08625

In cooperation with

Rutgers, The State University of New Jersey
And
Federal Aviation Administration (FAA)
And
U.S. Department of Transportation
Federal Highway Administration

Disclaimer Statement

The Center for Advanced Infrastructure and Transportation (CAIT) is a Regional UTC Consortium led by Rutgers, The State University. Members of the consortium are Atlantic Cape Community College, Columbia University, Cornell University, New Jersey Institute of Technology, Polytechnic University of Puerto Rico, Princeton University, Rowan University, SUNY - Farmingdale State College, and SUNY - University at Buffalo. The Center is funded by the U.S. Department of Transportation.

1. Report No.	2. Government Accession No.	3. Recipient's Catalog No.
CAIT-UTC-REG 30		

4. Title and Subtitle	5. Report Date
Durable and Electrified Pavement for Dynamic Wireless Charging of Electric Vehicles	August, 2022
	6. Performing Organization Code CAIT/ Rutgers, The State University of New Jersey

7. Author(s)	8. Performing Organization Report No.
Hao Wang, PhD https://orcid.org/0000-0001-8666-6900 Lukai Guo, PhD https://orcid.org/0000-0003-1727-5740	CAIT-UTC-REG 30

9. Performing Organization Name and Address	10. Work Unit No.
Department of Civil and Environmental Engineering Rutgers, The State University of New Jersey Piscataway, NJ 08854	11. Contract or Grant No. 69A3551847102

12. Sponsoring Agency Name and Address	13. Type of Report and Period Covered
Center for Advanced Infrastructure and Transportation Rutgers, The State University of New Jersey 100 Brett Road Piscataway, NJ 08854	Final Report 12/01/2019 – 12/31/2021
	14. Sponsoring Agency Code

15. Supplementary Notes
U.S. Department of Transportation/OST-R
1200 New Jersey Avenue, SE
Washington, DC 20590-0001

16. Abstract

As electric vehicles (EVs) tend to replace conventional gasoline vehicles, efficiently charging EVs with limit energy loss is critical. One promising solution is to utilize wireless charging module embedded in the pavement for dynamic charging. This study proposes an innovative design of partially magnetized pavement to improve the WPT efficiency via creating a magnetized pathway through the pavement layer. The specific magnetized area and location will be varied by the particular coil design. The basic WPT system with coils in air was first simulated and the results were validated by analytical solutions and experimental results. Finite element models (FEMs) of WPT-roadway systems were then built to analyze magnetic field and WPT efficiency of new design considering different coil embedment depth, vehicle wandering, magnetic properties of pavement layer. The results revealed the advantage of the partially magnetized pavement over conventional pavement for wireless power transfer, which did provide 1.5% ~ 13.3% improvement of charging efficiency. Such advantage from partially magnetized pavement was more significant if that surface layer above transmitting coil was thicker or the magnetized part had higher magnetic permeability. Moreover, the efficiency improvement remained effective until the vehicle lateral wander reached 0.5 m. The economic analysis showed that a high electricity cost saving was brought with limited amount of magnetic materials needed.

17. Key Words	18. Distribution Statement
Dynamic wireless charging; partially magnetized pavement; charging efficiency; finite element model; permitvity	

19. Security Classification (of this report)	20. Security Classification (of this page)	21. No. of Pages	22. Price
Unclassified	Unclassified	Total #32	

Form DOT F 1700.7 (8-69)

Acknowledgments

The authors would like to acknowledge the financial support provided by Center for Advanced Infrastructure and Transportation (CAIT) through the University Transportation Center Program.

Table of Contents

List of Figures

List of Tables

INTODUCTION

Although the development of battery technologies boosts uses of electric vehicles (EVs) in recent for cutting carbon intensity worldwide (Huang et al., 2021), one big challenge from efficiently charging those EVs still remains to limit the market share of EVs against conventional gasoline vehicles. Meanwhile, the charging time is still much longer than the time spent at regular gasoline station, even the time duration of charging an EV can be shortened from 8 hours to 35 minutes at fast charging stations. One of the alternative solutions to reduce charging time for drivers spent on stations is to use a charging system integrated in the roadway for complementarily charging the EVs when they are moving (Shin et al., 2013). Under this purpose, wireless power transfer (WPT) systems have been developed to be integrated into roadways, with acquiring promising efficiency (83% ~ 92%) and charging distance (10 cm ~ 200 cm) in 2010s (Kalwar et al., 2015). Among different WPT technologies, inductively coupled power transfer method (ICPT) is the most ideal option as a high-efficient wireless charging method when there is relatively large air gap between EVs and pavement.

The principle behind ICPT relies on the electromagnetic induction phenomena to transfer power between two coils through the air: the transmitter coil creates an alternative magnetic field by alternative currents; then, the alternative magnetic field is transmitted to the receiver coil through medium(s); in the end, the receiver coil generates alternative currents by the alternative magnetic field. Two resister-inductor-capacitor (RLC) resonant circuits are required to be respectively connected with transmitter and receiver coils, which are also coupled to produce electrical resonance at a system level, as shown in Figure 1. The use of ICPT can elevate the WPT efficiency to 83% ~ 92%, and meanwhile, it can extend the wireless charging distance to a significant further level (40 cm) (Kalwar et al., 2015).

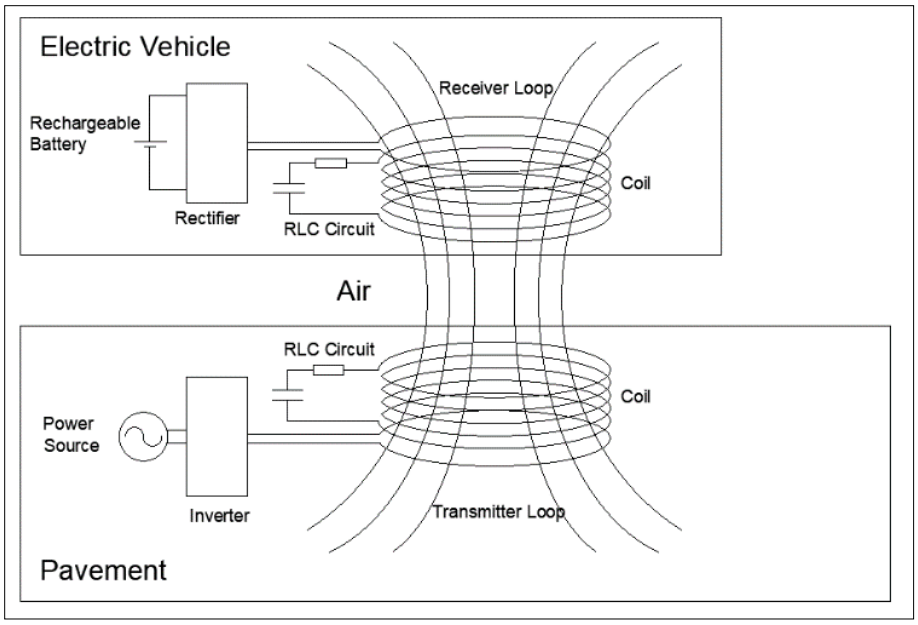

Figure 1 Database of pavement sections evaluated with different condition indexes

Most previous studies of ICPT system mainly focus on designs of electric coil and ferrite, electric circuit, and power electronics converters and control methods. However, besides the above factors purely from the electrical engineering side, the existence of pavement will inevitably affect the WPT efficiency between the coils in multiple ways. First of all, for preventing the transmitter coils from being worn under traffics, the coils cannot be directly exposed on the roadway surface, while placing them under the pavement surface layer can increase its distance away from receiver coils and reduce the WPT efficiency. Secondly, the dielectric loss factors of pavement construction materials can be significantly raised once the roadway gets wet on rainy days (Jonah and Georgakopoulos, 2012; Chen et al., 2017; Venugopal et al., 2018), which means more electromagnetic propagation loss may occur during wireless power transfer. Thirdly and most importantly, the existed pavement construction can lead to frequency mismatch which needs to be avoided in the coupled RLC circuits to maximize the WPT efficiency (Hsu et al., 2009; Moon et al., 2014; Chen et al., 2017; Sun et al., 2020).

A few studies have been conducted recently to integrate WPT into roadway pavement. Gardner (2017) modified a typical WPT system to be more suitably embedded into the concrete structure in the laboratory while remaining the promising WPT efficiency. It was observed that a coating thickness of at least 0.029 inches around the wire can keep the WPT system with the same electricity properties before and after embedment in concrete. Specifically, the inductance was

remained around 128 μH and the resistance was at 0.04 Ω. Based on the four-point bending test, the aluminum shielding plate, which was used to save the magnetic flux loss, was also suggested to be removed considering its negative impact on fatigue strength of the WPT-concrete structure. Cirimele et al. (2019) installed transmitting coil in concrete pavement and measured the amplitude and phase of coil impedance by LCR meter before and after embedment. It was found that the impedance of the device was not affected by the existence of concrete at low working frequency around 50 kHz. The results from numerical analysis showed that the resistivity of concrete, rather than the relative permittivity, significantly affected the overall performance of WPT system. This study also suggested to increase the thickness of insulating materials which covered the wire in the coil.

Some other studies tried to modify pavement material properties for improving the efficiency of WPT system. Edwards et al. (2019) blended dry powders (Portland cement, fly ash, sand, and magnetic powder) with some conductive additives (stainless steel wool, stainless steel fiber) to create a magnetizable cement mortar matrix in various core geometries and coil winding configurations. The peak flux, differential and impedance relative magnetic permeability, flux losses, and hysteresis power losses of totally 21 different mix combinations were measured and statistically analyzed. As results, it was found that, once the inclusions reached to a fraction level of 20%, the flux leakage and the hysteresis core loss of the mortar were both reduced by 50%, while the peak flux of mortar increased by 30% to 100% based on the coil winding. As an optimal solution, a steel reinforced magnetic concrete core, which contains 20% of ferritic fiber and powder inclusion, caused peak flux of 100 mT and relative permeability of 28. Mahmud et al. (2017) proposed one WPT system that used the cement modified by nano-magnetics materials that can be used as roadway surface. The content of additives was either 10% iron or 20% magnetite. As a result, a 13-A output current was obtained from a 15-A input current under 50 kHz, which indicated 86% efficiency of WPT. Venugopal et al. (2018) found that adding an inductive layer of asphalt (treated by graphite or steel wool) between two coils within the WPT did not significantly reduce the WPT efficiency unless the alternative current reached high frequency. Specifically, the efficiency dropped below 90% once the frequency of alternative current was raised to be 100 kHz. That study also replaced the asphalt layer by a solar panel to be sandwiched by the primary and secondary coils. It was found the combined system of WPT with solar panel did not work well if the frequency reached beyond 10 kHz due to the eddy currents induced in the solar panel. However,

most previous studies did focus on testing and modifying pavement materials to quantify and mitigate their negative impacts on WPT efficiency, while did not specify the corresponding pavement structure changes with (partially or fully) filling those modified pavement construction materials for improving the WPT efficiency in roadway system.

OBJECTIVE AND SCOPE

This study proposes an innovative design of partially magnetized pavement layer to increase the efficiency of WPT system from roadway to EVs. The basic principle behind this design is to create a pathway for better guiding the magnetic flux between electric coils through a specially designed pavement layer, with also avoiding any short circuits of magnetic field inside the pavement layer. This study develops numerical simulation models to observe the magnetic flux changed by the pathway for proving such magnetic flux improvement. Moreover, the WPT efficiency is estimated for quantifying the specific energy saving percentage under different scenarios. It is worth noting that circular coils are selected as an example in this study for quantifying the benefit of wireless power efficiency and potential energy saving from the proposed partially magnetized pavement design principle, while the circular coil design is not the only suitable option for this proposed design principle. The electrified pavement shall be adjusted based on the specific design of charging module and coil configuration.

DESIGN PRINCIPLE OF PARTIALLY MAGNETIZED PAVEMENT

In general, there are two major strategies to mitigate the negative impacts on WPT efficiency from pavement construction materials. First strategy is to modify magnetic properties of pavement layers by adding magnetic materials, which is the one adopted by previous studies. However, overusing magnetic materials may make the pavement layer being as a magnetic shield. The alternative magnetic field generated by the transmitter coil will be therefore trapped inside the pavement, although it can be utilized for heat-induced self-healing of asphalt pavement (Liu et al., 2020).

Another strategy is to create pathways through the pavement layer for guiding the magnetic field between transmitter and receiver coils, which is the one proposed and focused in this study. The pathway is made by forming a partially magnetized pavement layer, as shown in Figure 2.

The detailed structural design of the pathway follows the path of magnetic field, which can be further varied based on the coil size and configuration. As can be seen from Figure 2, the magnetic field will be not connected in short circuit through the pavement layer due to the cut from the regular pavement between magnetic layers in vertical direction. The pathways through the pavement are expected to better guide magnetic flux between coils and cause less energy loss due to its overall improvement of magnetic permeability.

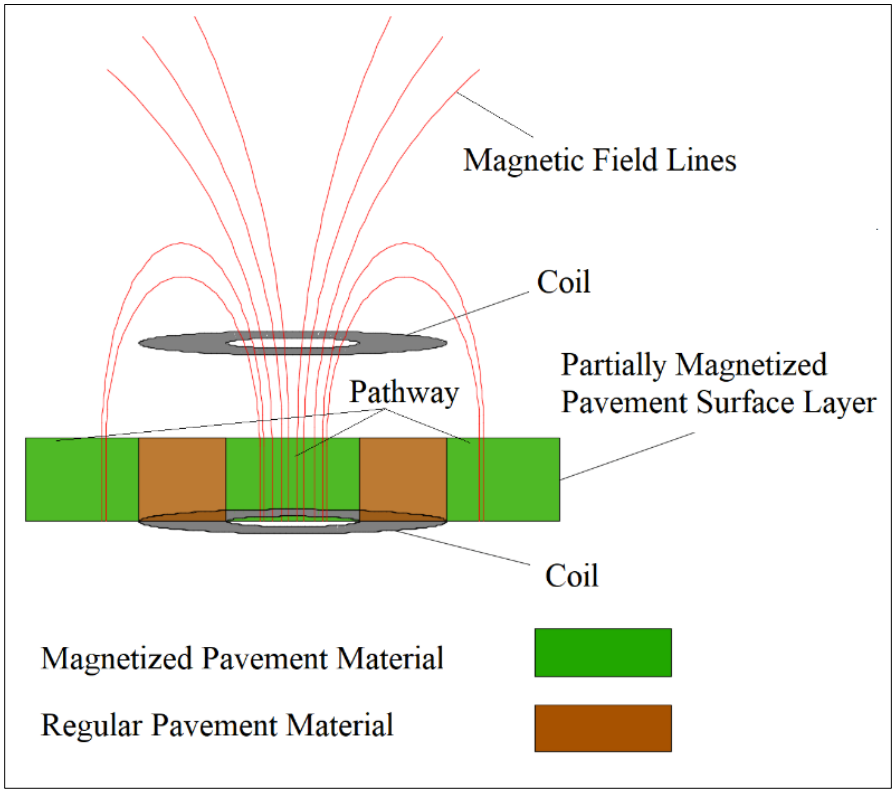

Figure 2 Design concept of partially magnetized pavement layer

DEVELOPMENT AND VALIDAITON OF NUMERICLA MODEL

Analytical Solution of Basic WPT System

The electrical circuits in basic WPT system mainly include the equivalent series resistances of transmitting and receiving coils, R_1 and R_2, one load resistance, R_L, a power supply with high frequency current (or voltage), i_s (or u_s), the series capacitances, C_1 and C_2, and the inductances of transmitting and receiving coils, L_1 and L_2, as shown in Figure 3. The electric currents flowing inside transmitting and receiving coils are respectively labeled as i_1 and i_2. A system of capacitors

and inductances (coils) is able to create electrical resonance with limited energy loss, similar to a spring system under vibration. With current flows through both coils, the coils can further be treated as two magnets in the magnetic field.

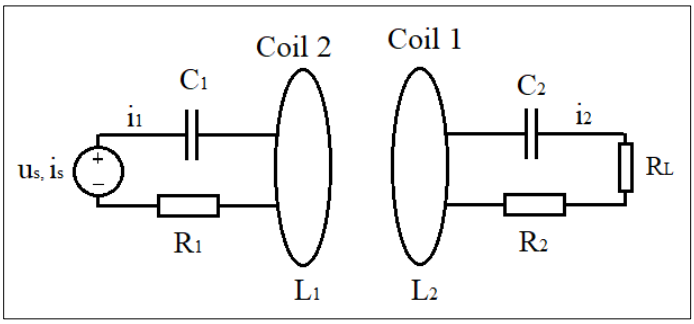

Figure 3 Equivalent circuit model of two-coil WPT system

Based on Kirchhoff's voltage law, the equivalent circuit model can be expressed in Equation 1 and 2.

$$\left(-j\frac{1}{\omega C_1}+j\omega L_1+R_1\right)i_1-j\omega M i_2=u_s \tag{1}$$

$$\left(-j\frac{1}{\omega C_2}+j\omega L_2+R_2+R_L\right)i_2-j\omega M i_1=0 \tag{2}$$

Where, ω is the angular frequency; j is the imaginary unit; and M is the mutual inductance between coils.

Once the transmitting and receiving coils are both under resonant states and their resistances both equal to *R*, Equation 1 and 2 can be further rewritten into Equation 3 and Equation 4.

$$Ri_1-j\omega M i_2=u_s \tag{3}$$

$$(R+R_L)i_2-j\omega M i_1=0 \tag{4}$$

The system transfer efficiency, η, can be written in Equation 5.

$$\eta=\frac{P_{out}}{P_{in}}=\frac{R_L}{(R+R_L)\left(1+\frac{R(R+R_L)}{(\omega M)^2}\right)} \tag{5}$$

As can be seen from Equation 5, the transfer efficiency of WPT is mainly determined by two major features from coils, including their resistances, *R*, and their mutual inductance, *M*. Meanwhile, if the coils are unchangeable, the maximum transfer efficiency can be reached by adjusting the load resistance, R_L, and the angle frequency, ω.

The total resistance of coils is counted by its ohm resistance, R_0, radiant resistance, R_r, and the resistance due to skin effect, R_s. This group of resistances can be respectively calculated through Equation 6 to Equation 8 (Dong et al., 2018). As can be seen from those equations, the ohm resistance is mainly determined by the material and the geometric features of coils, including the electrical conductivity of coils, σ, the number of coil turns, *N*, the mean coil radius, *r*, and the cross section radius of wire, *a*. Compared to ohm resistance, the radiant resistance is additionally decided by the light speed, c, which makes the resistance value ignorable at this level of estimation. Besides those two resistance types, within this two-coils system, a skin effect can be a considerable factor affecting the power transfer efficiency with an additional factor, skin depth, $\delta = \sqrt{\frac{2\rho}{\omega\mu}}$.

$$R_0 = \sqrt{\frac{\mu_0\omega}{2\sigma}}\frac{Nr}{2a} \tag{6}$$

$$R_r = \sqrt{\frac{\mu_0}{\varepsilon_0}}\left[\frac{\pi}{12}N^2\left(\frac{\omega r}{c}\right)^4 + \frac{2}{3\pi^3}\left(\frac{\omega h}{c}\right)^2\right] \tag{7}$$

$$R_s \approx \frac{L\rho}{2\pi r\delta} \tag{8}$$

Where, ρ is the resistivity of the coil; μ is the permeability of the coil; μ_0 is the permeability of the free space, L is the length of coil; ε_0 is the permittivity of free space; and h is the height of a spiral coil.

A general equation to determine the mutual inductance between coils can be expressed in Equation 9 after the inductances of coils, L_1 and L_2, and the coefficient of coupling, *k*, are known.

$$M = k\sqrt{L_1L_2} \tag{9}$$

For circular coils, the coefficient of coupling, *k*, is strongly correlated to the distance of coils, *D*, and their radius, r_1 and r_2, as shown in Equation 10 (Lu et al., 2020).

$$k = \frac{1}{\left[1+2^{2/3}(D/\sqrt{r_1 r_2})^2\right]^{3/2}} \quad (10)$$

Comparison between Results from Analytic Functions and FEMs

For the verification purpose, the same basic WPT system consisting of two coils with an air-only transmission medium is evaluated using both analytic functions and numerical solutions. The specific coil design used in this WPT system is made by copper with an average radius of 0.5 m (inner radius of 0.2 m and outer radius of 0.8 m), a cross-section radius of 1.5 mm, and 20 number of turns. On one side, a current source of 20 Å is connected with the transmitter coil. On another side, a load resistance of 20 Ω is connected with the receiver coil. Moreover, to achieve electrical resonance on both transmitter coil and receiver coil, two 1.3-μF capacitors are individually added in transmitting and receiving electrical circuits under an alternating current frequency of 75 kHz.

Based on the outputs from FEM of the basic WPT system, the transfer efficiency can be calculated as the ratio between powers inside these two coils. In addition, the coil characteristics (resistance, R, and inductance, L1 and L2) can be achieved via coil geometry analysis in the numerical model. After inputting these coil characteristics, accompanying with other given parameters (load resistance, RL, overall radius, r, operational frequency, ω, coil distance, D), the efficiency of this basic WPT system can be calculated from analytical solutions (Equation 5, 9 and 10).

The WPT efficiencies of the basic WPT system calculated from FEM and analytic functions in various coil distances (from 0.1 m to 0.5 m) are displayed in Figure 4. In general, the results from numerical solution and analytic function are consistent with each other. If the coil distance is as close as 0.1 m, the WPT efficiencies from both calculation methods are consistently around 95%. Once the coil distance gradually increases to 0.5 m, the WPT efficiencies drop noticeably, although slight differences are found between FEM and analytic solutions. This difference can be caused by the magnetic flux simulated by FEMs which is closer to the real case with less of them crossing both coils in a longer gap, while the analytic solution is based on a more ideal scenario.

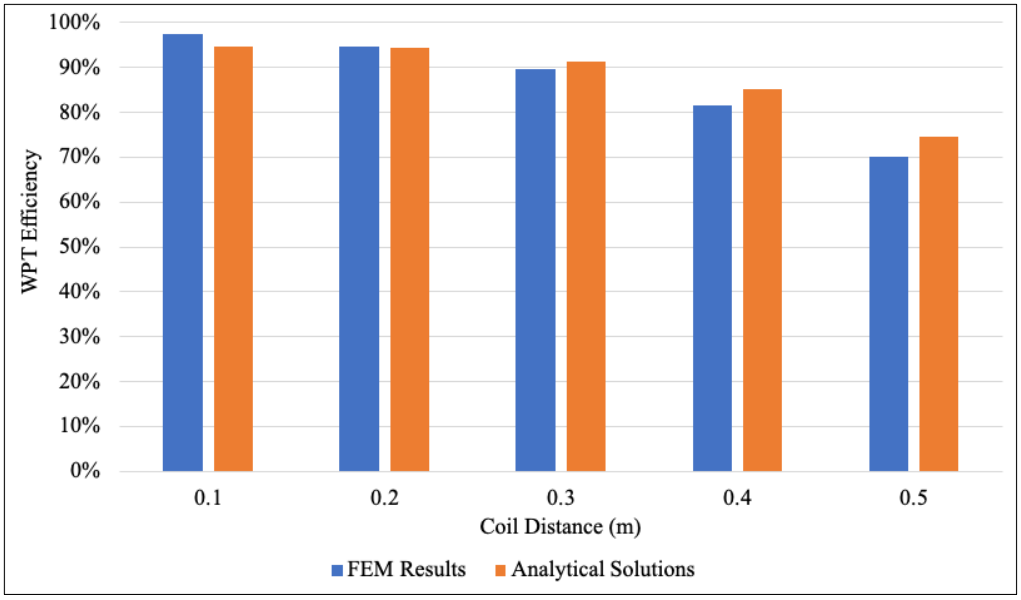

Figure 4 Comparison of Results from FEM and Analytical Solutions

Comparison between Results from Laboratory Tests by Previous Study and FEMs

To further ensure the accuracy of FEMs built in this study, laboratory testing results measured by one previous study (Li et al., 2021) are used for comparing the corresponding FEM results obtained from this study. In the laboratory testing part of that previous study, asphalt concrete specimens (AC) were placed between primary coil and secondary coil in turn. The size of each coil was in a diameter of 1.65 mm with 40 turns, with ferrite slabs on the back. The coil distance was fixed at 60 mm. An output voltage of 15 V in a resonant frequency of 87 kHz was supplied to the primary coil and wirelessly transmitted to the secondary coil. As a result, a maximum of 83.7% power transmission efficiency was captured while one asphalt concrete specimen was placed between coils (Li et al., 2021).

On verification purpose, the corresponding FEM with coils and asphalt concrete specimens in the same size are built through revising the original FEM developed by this study, as displayed in Figure 5. The schematics of FEMs are remained the same, expect of some detailed design parameters of coils and asphalt concrete specimens. In addition, since the laboratory tests conducted by previous study add ferrites behind coils, the corresponding FEM built by this study also involves ferrites cooperating with coils. As a result, under an output voltage of 15 V in 87 kHz, a transmission efficiency of 84.7% is obtained from the FEM, which is within ±1% difference

from the laboratory testing result observed by previous study. The close transmission efficiency estimated from FEM built by this study against the one directly measured from laboratory tests by previous study further confirms the reliability of FEM results calculated in this study.

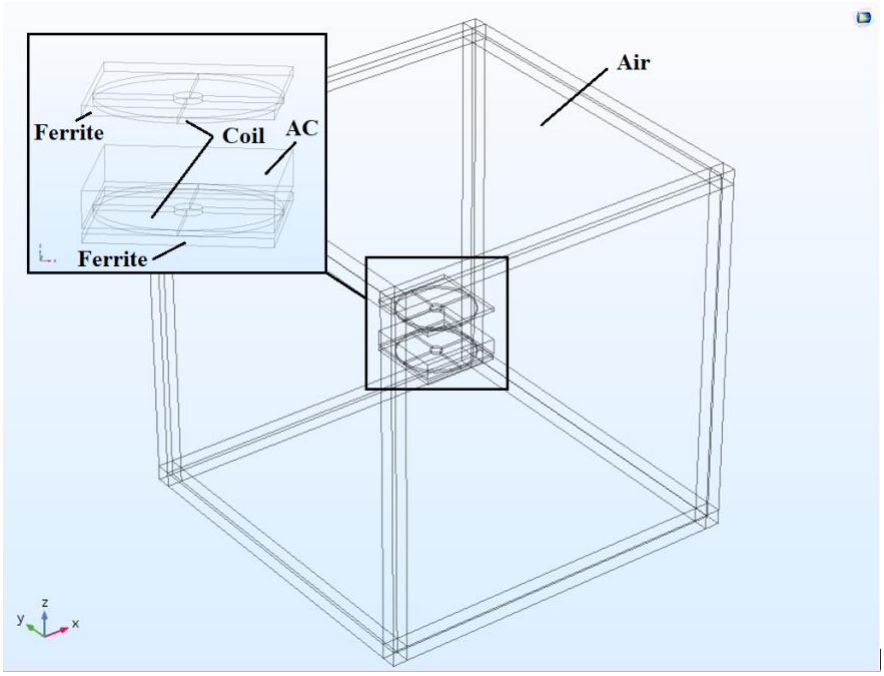

Figure 5 Revised FEM on Simulating Laboratory Tests by Previous Study

FINITE ELEMENT MODELS OF WPT IN CONVENTIONAL AND PARTIALLY MAGNETIZED PAVEMENT

The FEM of WPT system embedded in the pavement is built using COMSOL software. The model consists of two coils (one in air and another under pavement layer), one asphalt layer, and an air space. The COMSOL modules involved in this FEM include a Magnetic Fields module and an Electrical Circuit module. The geometrics of entire basic wireless charging roadway is displayed in Figure 6. The pavement section with one traffic lane is modeled in a width of 3.6 m and a length of 2 m in traffic direction. The transmitter coil is embedded at a depth of 0.1-0.4 m under the pavement surface, while the receiver coil on EVs is placed above the pavement surface at a height of 0.4 m. Another 0.2 m-thick base layer is placed under transmitter coil as part of pavement structure. The material properties of different components used in FEM for wireless charging simulation are listed in Table 1.

Table 1 Material properties of components in wireless charging pavement

	Relative Permeability	Relative Permittivity	Electrical Conductivity	Reference
Air	1	1	0	COMSOL default
Pavement	1	5.3	0	Pellinen et al., 2015; Wang et al., 2019
Coil (copper)	1	1	6×10^{7}	COMSOL default

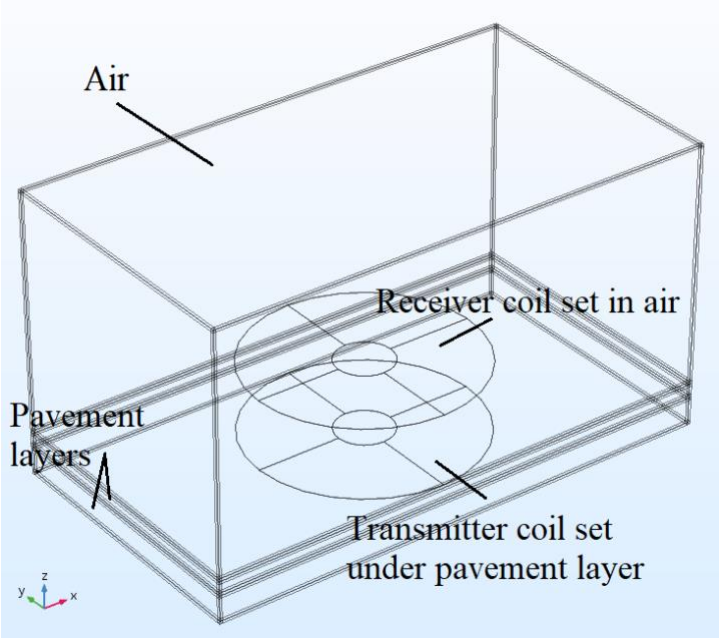

Figure 6 Illustration of WPT System in Conventional Pavement

For all electric components involved in the simulation, only coils are physically added in geometrics, while other electronic components are assembled in the Electric Circuit module. For geometric features of coil, the radius of coil is assumed as 0.5 m, which is consistent that used by previous studies (Miller and Daga, 2015; Dong et al., 2018). Other basic features of coils, such as the number of turn and the cross-section area, are defined in the Magnetic Fields module, respectively as 20 and 1×10^{-6} m^2.

As above mentioned, to improve the WPT efficiency, a partially magnetized pavement layer, consisting of traditional pavement materials and a magnetized material, is proposed in this study. Figure 7 shows the WPT system integrated with magnetized pavement, where the area covered by magnetized materials is marked blue. The specific material properties used in the model are consistent with those listed in Table 1, except for the magnetized pavement material. Based on the measurements from previous studies, the electric conductivity and the relative permeability of a magnetized pavement material with 20% magnetite additives are set as 0.1 S/m and 150, respectively (Mahmud et al., 2017). Given the relative permittivity of ferrite powder is close to the air (Li et al., 2020), the relative permittivity of magnetized pavement material is assumed to be 5.6, which is close to that of conventional pavement material (Wang et al., 2019).

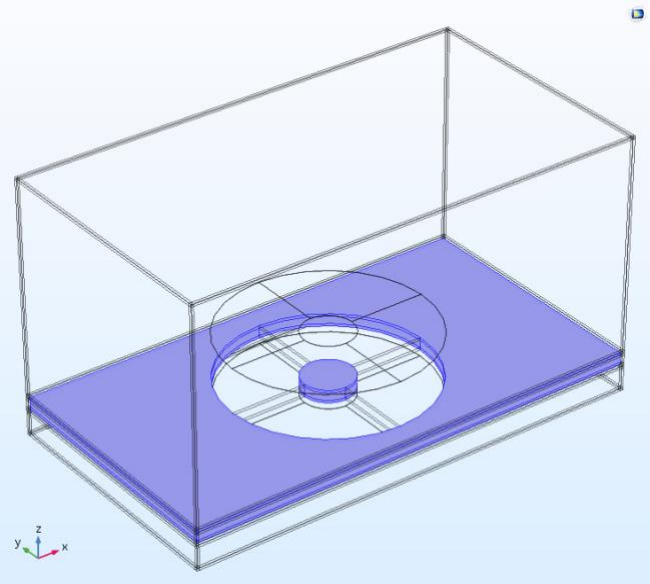

Figure 7 Illustration of WPT System in Partially Magnetized Pavement Layer

SIMULATION RESULTS AND DISCUSSIONS

Effect of Magnetized Pavement Layer on Magnetic Field

The hypothesis behind partially magnetized pavement layer proposed in this study relies on the pathway created within the pavement surface made by magnetized materials. The change of magnetic flux distribution before and after adding the partially magnetized pavement layer needs to be captured to prove the hypothesis. The simulation results of WPT system with a conventional pavement layer and the WPT system with a partially magnetized pavement layer are then compared

and analyzed at this section. At first simulation step, the thickness of pavement layers above the transmitter coil are initially set as 0.1 m and the distances between transmitting and receiving coils are set as 0.5 m. As results, the magnetic flux distributions within these two WPT systems are shown in Figure 8.

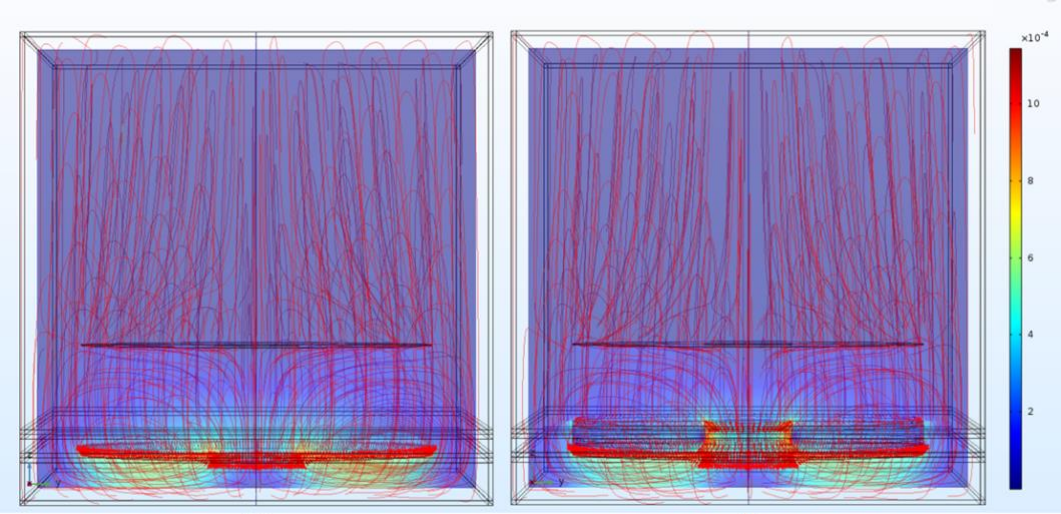

Figure 8 Magnetic field distribution (magnetic line in red) of WPT systems for coils under (a) conventional and (b) partially magnetized pavement layer at 0.1-m depth

Since the magnetic flux density expressed via magnetic lines and arrows plotted in Figure 8 is magnitude controlled, the higher density of magnetic lines and the longer length of arrows reflect the higher strength of magnetic field. The results from Figure 8 show that the strongest magnetic field is created by the transmitter coil under the pavement layer. Once the magnetic flux passes a conventional pavement layer, the magnetic field strength is dispersed. However, as the magnetic flux passes a partially magnetized pavement layer, the magnetic field remains certain strength through the pavement layer.

To more clearly observe the affect from existence of partially magnetize layer on better guiding the magnetic flux for improving WPT efficiency, the thickness of partially magnetized pavement layer is further increased from 0.1 m to 0.4 m for better capturing the magnetized pathway. As can be seen from Figure 9 (a) and (b), a strong magnetic field does penetrate through the pathway created by the partially magnetized pavement layer with remaining its strength, while the magnetic field is scattered and weakened if it is not guided by any magnetized pathway through

conventional pavement layer. Based on those different magnetic flux distributions, the feasibility of improving WPT efficiency via creating a pathway to guide the magnetic field passing over the pavement layer is visibly demonstrated. The partially magnetized pavement layer is as transforming of an original pavement surface layer to an additional ferrite component between the coils. This type of transformation can also be implemented under other similar circumstances that a medium inevitably needs to be between coils and if the medium can be partially magnetized.

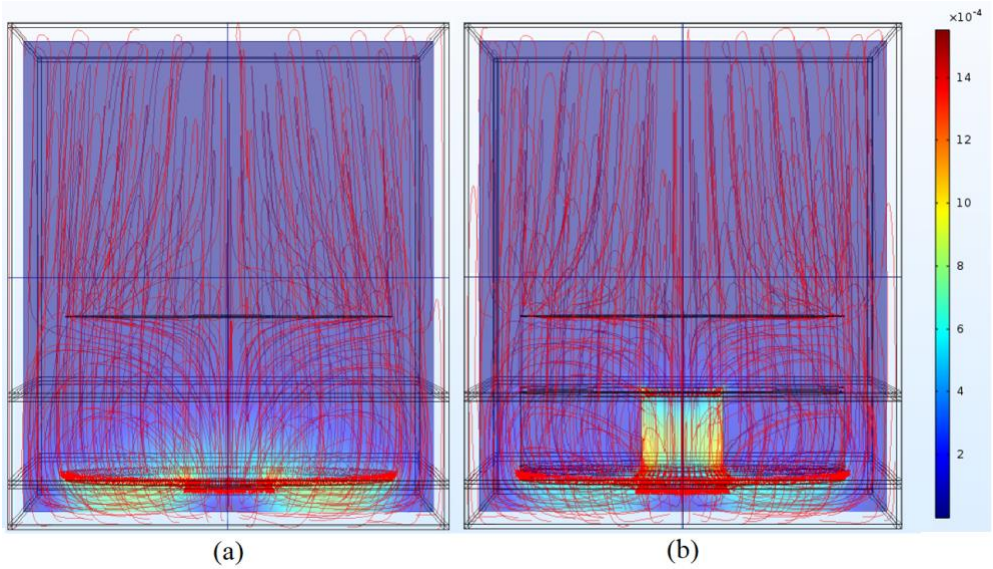

Figure 9 Magnetic field distribution (magnetic line in red) of WPT systems for coils under (a) conventional and (b) partially magnetized pavement layer at 0.4-m depth

Effect of Magnetized Pavement Layer on WPT Efficiency

Since the advantage of this partially magnetized pavement layer mainly relies on the pathway, which can better connect the magnetic flux between upper and lower coils, the length of pathway shall affect the improvement of WPT efficiency. Intuitively, if the distance between transmitting and receiving coils needs to be longer, adding the partially magnetized layer can more significantly mitigate the negative impact of the distance on WPT efficiency. To verify this point and quantify the consistency of WPT efficiency improvement under different surface layer thicknesses over the transmitter coil, the WPT system with partially magnetized and unmagnetized pavement layers are respectively built in a wide range of surface layer thicknesses (0.1 m to 0.4 m). The transmitter coil is placed exactly below the pavement surface layers at a depth varying from 0.1 m to 0.4 m;

while the receiver coil is remained above the pavement surface at a height of 0.4 m (assuming the location of receiver coil on the electric vehicle is not changed).

The WPT efficiencies from partially magnetized pavement layer and conventional layer are calculated for different thicknesses of magnetized pavement layer above the transmitter coil that is the same as the embedment depth of transmitter coil, as shown in Figure 10. As expected, for either partially magnetized or unmagnetized pavement layer, the WPT efficiency gradually decreases as the transmitter coil is getting deeper with the thicker surface layer. However, the advantage from partially magnetized pavement layer on improving WPT efficiency is more significant when the surface layer above the transmitting coil gets thicker. As the depth of transmitter coil increases from 0.1 m to 0.4 m, the improvement of WPT efficiency increases from 1.5% (71.5% vs. 70.1%) to 12.3% (39.9% vs. 27.6%) due to the partially magnetized layer. Moreover, the deduction of WPT efficiency by increasing each 0.1-m transmission coil depth is approximately -10% for partially magnetized layer versus -15% for normal layer, which also reflects the mitigation function against WPT efficiency deduction from the partially magnetized layer over regular pavement layer. These findings indicate that the advantage brought by the partially magnetized layer is more significant when the wireless charging module needs to be embedded deeper in the pavement structure to prevent load-induced damage and increase the system longevity (Jasim et al. 2019).

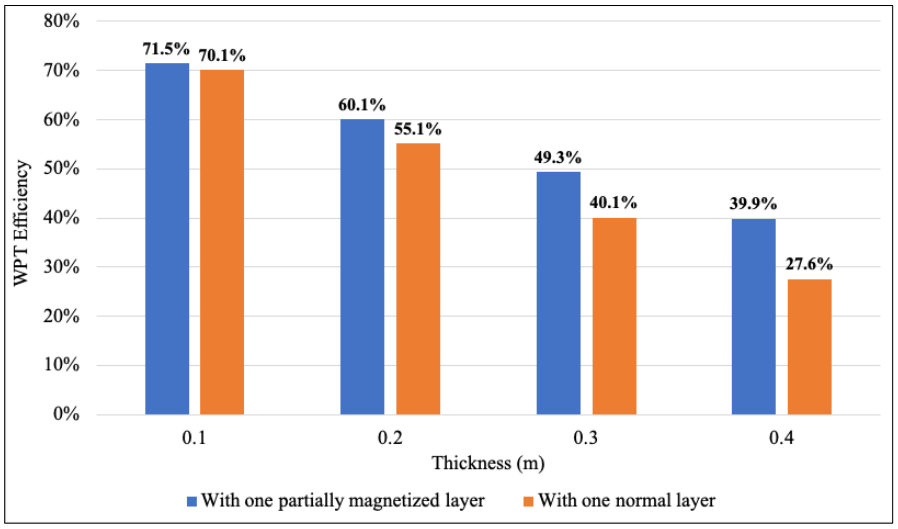

Figure 10 WPT efficiencies at different thicknesses of conventional and magnetic pavement layer above the transmitter coil

Effect of Vehicle Wandering on WPT Efficiency

Vehicle wandering is a common phenomenon for human driving vehicles due to the uncertainty of lateral position of wheels in traffic lanes. Considering that lateral offsets between transmitter and receiver coils will occur due to wandering of electric vehicles, the advantage from partially magnetized layer on WPT efficiency under vehicle wandering scenarios needs to be checked.

Figure 11 shows the calculated efficiencies of WPT systems with different lane deviation by vehicle wandering between transmitting and receiving coils (0, 0.15, 0.25, and 0.5 m). For comparison purpose, the same coil configurations are simulated with a conventional pavement layer as the baseline. As can be seen, for both layer designs, the WPT efficiencies are decreased as the lane deviations are enlarged, but not exactly linearly: a 27% of dramatic WPT efficiency drop occurs when the lane deviation is increased from 0.25 m to 0.5 m. Meanwhile, the advantage of partially magnetized pavement layer on WPT efficiency improvement remains if the coil offset reaches to 0.25 m. However, once the coil offset is further increased to 0.5 m, such WPT efficiency improvement from the partially magnetized pavement layer can be eliminated. This can be caused by a short-circuit magnetic flux: once the receiver coil is deviated from centerline, the pathway of magnetic flux through pavement layer can be cut by a fully magnetized area above the transmitter coil. Given the average lane deviation by vehicle wandering is about 0.15 m (0.5 ft) (Chang et al., 2019), the advantage from this partially magnetized pavement layer on WPT efficiency improvement will most likely be remained.

Under a 0.15-m average driver lane deviation scenario, Figure 12 displays the WPT efficiencies changed by the thickness of conventional or partially magnetized layers above the transmitter coil. The results reflect that, the WPT efficiency differences under zero and 0.15-m lane deviation scenarios remains 2% ~ 3% level of difference, regardless the varied thickness of the partially magnetized layer. This finding shows no interaction between lane deviations and layer thicknesses on the WPT efficiency improvement. In other words, for a WPT system at any specific layer thickness, its WPT efficiency under 0.15-m lane deviation can be predicted by deducting 2 to 3 percentages from the WPT efficiency measured under no lane deviation.

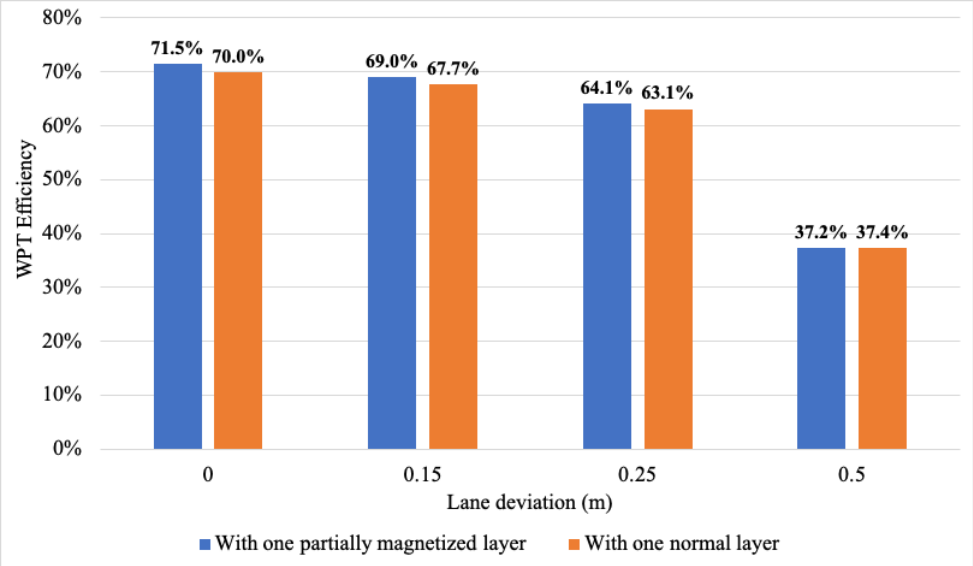

Figure 11 WPT efficiencies at different lane deviations by vehicle wandering with 0.1-m conventional and magnetized pavement layer

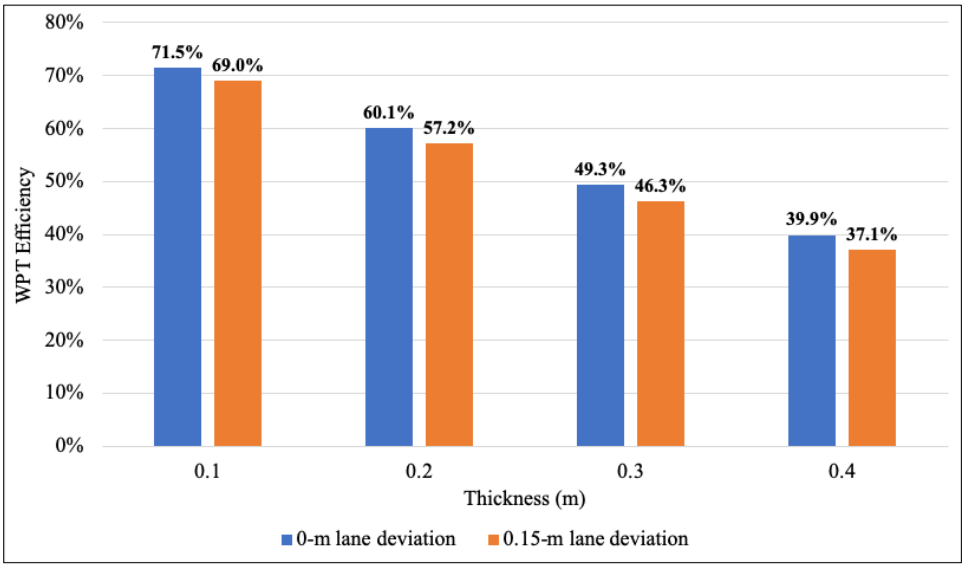

Figure 12 WPT efficiencies at different thicknesses of partially magnetized pavement layer with or without 0.15-m lane deviation

With counting the lane deviation affect, Figure 13 shows the WPT efficiency comparison between with or without partially magnetized pavement layers under a 0.15-lane deviation scenario. Similar as the results shown from Figure 10 without lane deviation involved, the one with partially magnetized layer can improve the WPT efficiency more significantly from 1% to 10% as its thickness is getting thicker from 0.1 m to 0.4 m. More importantly, with a 0.15-m lane

deviation, the drop of WPT efficiency by each 0.1 thickness increment is getting less for a partially magnetized layer while is oppositely getting more for a normal layer. Such opposite WPT efficiency drop results can be contributed by the magnetic field line changes due to the normal pavement layer being partially magnetized. This finding demonstrates that the WPT efficiency improvement created by the partially magnetized pavement layer will not only remain but boost if lane deviation occurs.

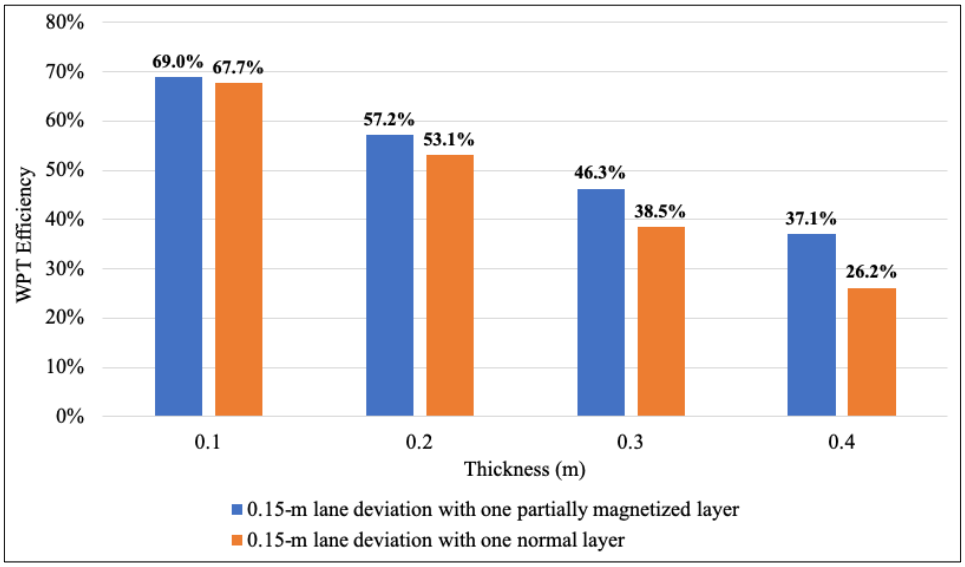

Figure 13 WPT efficiencies at different thicknesses of conventional and partially magnetized pavement layer with 0.15-m lane deviation

Effect of Permeability on WPT Efficiency

In theory, increasing the permeability of magnetized area can better control magnetic flux and further improve wireless charging efficiency. However, due to the limit length of the magnetic flux pathway due to the thickness of the pavement layer, such efficiency improvement from material property changes can be limited. To further study the effect of permeability of the magnetic flux pathway on the WPT efficiency, this section simulates the WPT system at two different thicknesses of partially magnetized pavement layer above the transmitter coil (0.1 m and 0.4 m) with several permeability levels in the magnetized area (from 1, 5, 10, 15, 30, 60, 100, to 150). The relevant WPT efficiency changes are then observed as the permeability is increased, as shown in Figure 14.

As can be seen from Figure 14, in general, the WPT efficiency increases as the permeability of magnetized pavement layer increases. However, with 0.1-m thickness of partially magnetized layer, the improving rate of 1% is limited (from 70.1% to 71.1%) and can be easily reached with a permeability of 15 from magnetized pathway. Previous work has found that adding 20% magnetic additives into cement can increase permeability to 150 (Mahmud et al., 2017), thus a much smaller content of magnetic powder is sufficiently needed to increase WPT efficiency by 1%. On the other hand, once the thickness of partially magnetized layer is increased to 0.4 m, the improving rate is significantly amplified to be 13.3% (from 26.6% to 39.9%) after the permeability of magnetized pathway reaches from 1 to 150. This result shows the effect of permeability on WPT efficiency improvement depends on the thickness of partially magnetized pavement layer.

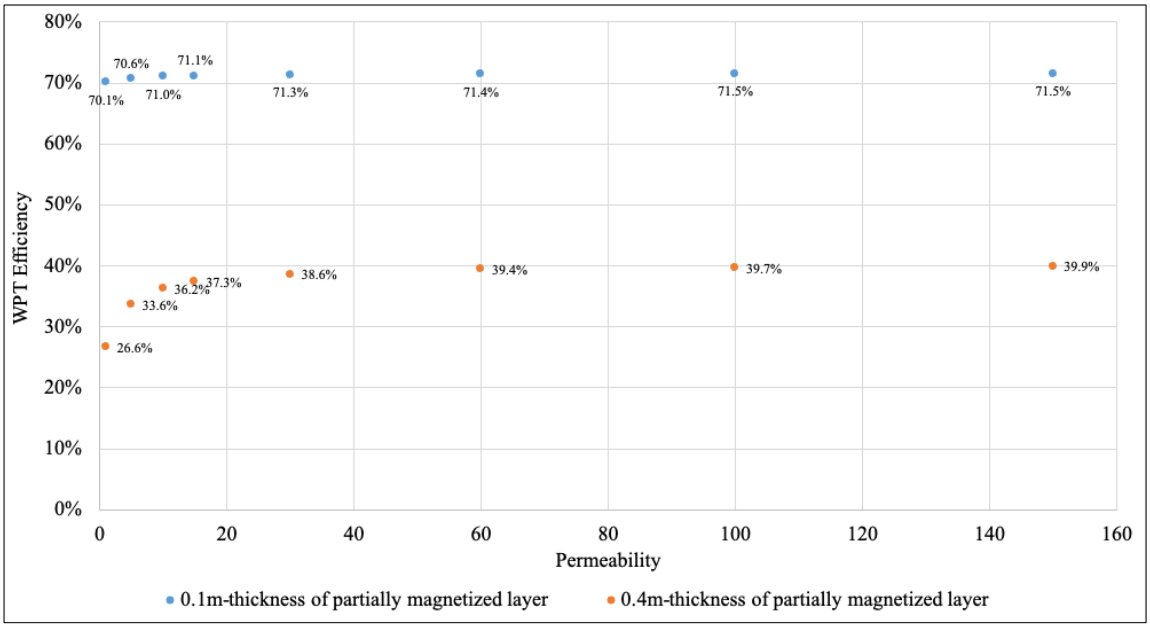

Figure 14 WPT efficiencies for partially magnetized pavement layer having different permeability values

ECONOMIC FEASIBILITY ANALYSIS

As shown in the results above, with 0.1-m partially magnetized pavement layer, around 1.5% improvement of wireless charging efficiency can be achieved. Although this level of percentage improvement is not too considerable, the total amount of energy saving from the partially magnetized pavement design can be accumulated and become significant over years. On practical

purpose of utilizing this partially magnetized layer in the field, this study estimates the electricity cost that can be saved over years from a 3.6 m × 2 m wireless charging pavement section with the proposed design. The electricity cost saving per year, *CS*, is calculated based on the total electricity saved per year with the unit cost of electricity, as expressed in Equation 11 (Shang et al., 2013). Over years, the present value, *PV*, is further calculated by accumulating the *CS* with considering the real discount rate, *r*, as shown in Equation 12. The real discount rate is estimated based on the social discount rate and inflation rate using Equation 13 (Lazzeroni et al., 2020).

$$CS = P \times t \times 365 \times C_e \times \Delta\eta \tag{11}$$

$$PV = \sum_{T=0}^{Y} \frac{CS}{(1+r)^T} \tag{12}$$

$$r = \frac{SDR - IR}{1 + IR} \tag{13}$$

Where, P is the power needed for wireless charging electric vehicles; t is the daily charging in hours; C_e is the unit cost of electricity; $\Delta\eta$ is the improvement percentage of wireless charging efficiency by partially magnetized pavement layer; T is number of years; Y is the service life of wireless charging pavement by years; SDR is the social discount rate; IR is the inflation rate.

Among all above parameters in Equation 11, the power for charging electric vehicles is assumed to be as constant value of 20 kW (Tavakoli and Pantic, 2017; Onar et al., 2018) at a speed of 95 km/h (Lazzeroni et al., 2020); the electricity price is fixed as an average cost level over United States as 0.12 $/kWh; the service life of wireless charging pavement is assumed to be 20 years, which meets the pavement design criteria; the social discount rate and the inflation rate in United States are respectively 7% and 2.1%. In practical, the specific operation hours of wireless charging from each wireless charging pavement section can be widely varied based on daily traffic volumes of electric vehicles. The specific WPT efficiency improvement, as found in this study, is dependent on the thickness of partially magnetized pavement layer and the permeability of its magnetized material.

With concerning the uncertainties from charging hours and the specific WPT efficiency improvement, this study estimates the range of electricity cost savings from the partially magnetized pavement layer, as displayed in Figure 15. As can be seen, the economic benefit from

each 3.6 m × 2 m partially magnetized pavement section can be from $167 to $17,700 if the WPT efficiency improvement is varied from 1.5% to 13.3% under different design scenarios and the daily charging time is extended from 1 hour to 12 hours. Assuming one-mile pavement section equipped with WPT, the cost saving would range from $0.2-14 million. This wide range of economic benefit can be further used as a threshold for deciding the maximum of total construction cost allowed for utilizing this partially magnetized pavement structure to make it profitable in the field.

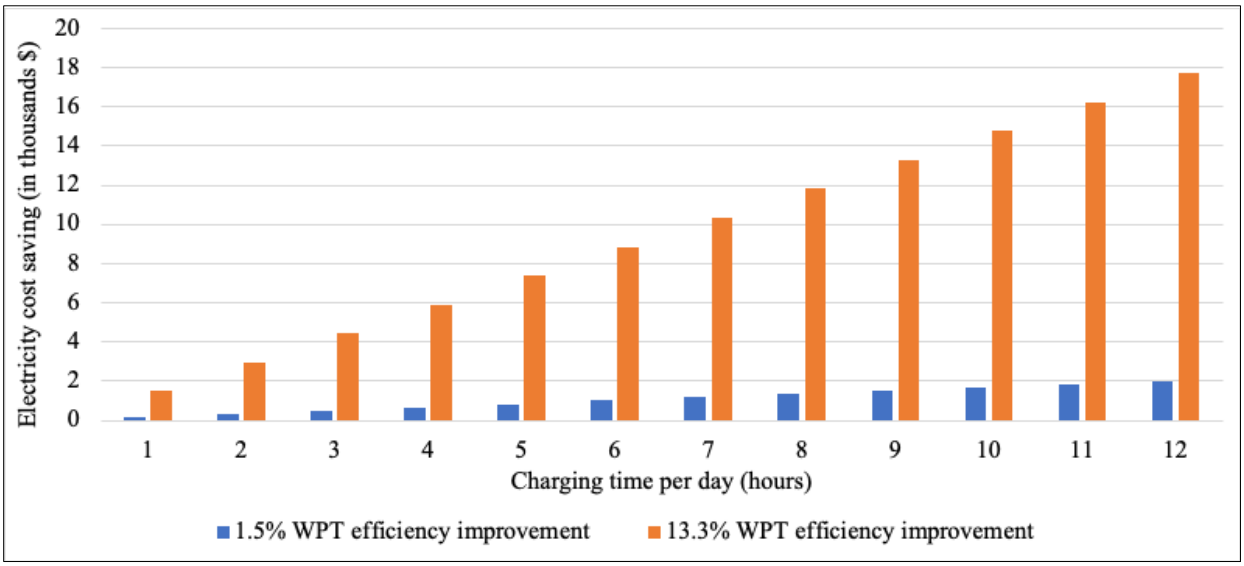

Figure 15 Electricity cost saving of each charging pavement section

CONCLUSIONS

Most previous studies make contributions on revising pavement materials or coil designs to mitigate the negative impact from pavement layer on wireless charging efficiency to the electric vehicles, while few of them realize that the pavement layer itself can be modified with the same function as ferrite to improve the wireless charging efficiency between coils. Regarding this point, this study proposes an innovative design of partially magnetized pavement to improve wireless charging efficiency from roadway to electric vehicles. The design principle is to create a pathway that can better guide magnetic flux and connect magnetic fields between transmitter and receiver coils. For quantifying technical benefits and economic feasibility of partially magnetized

pavement, the WPT efficiency of partially magnetized pavement and conventional pavement is analyzed using numerical simulation of WPT system in the pavement.

The analysis results reveal the improvement of wireless power transfer from partially magnetized pavement layer over conventional pavement layer for charging EVs. The wireless charging efficiency can be raised 1.5% from 70% to 71.5% if the embedment depth transmitter coil is 0.1 m. Such efficiency improvement can further increase to 12% if the pavement layer above the transmitter coil is getting thicker to be 0.4 m. Meanwhile, the efficiency improvement from this partially magnetized pavement layer is still effective until the vehicle deviates away from the center of driving lane by 0.5 m. The permeability of magnetized pavement layer has more significant effects on WPT efficiency when the transmitter coil is embedded at deeper depths. The specific electricity cost saving for one-mile partially magnetized pavement section can be ranged from $0.2-14 million, depending on the specific efficiency improvement and the daily charging hours of WPT system. Further study should be conducted to validate simulation results through prototype tests and considering more complex charging system designs.

REFERENCES

Chang, K., Ramirez, M., Dyre, B., Mohamed, M., and Abdel-Rahim, A., 2019. Effects of longitudinal pavement edgeline condition on driver lane deviation. *Accident Analysis & Prevention*, *128*, pp.87-93.

Chen, F., Taylor, N., Balieu, R. and Kringos, N., 2017. Dynamic application of the Inductive Power Transfer (IPT) systems in an electrified road: Dielectric power loss due to pavement materials. *Construction and Building Materials*, *147*, pp.9-16.

Cirimele, V., Torchio, R., Virgillito, A., Freschi, F. and Alotto, P., 2019. Challenges in the Electromagnetic Modeling of Road Embedded Wireless Power Transfer. *Energies*, *12*(14), p.2677.

Dong, Y., Lu, W., Liu, Y. and Chen, H., 2018, October. Optimal Study of Resonant Wireless Charging Coils for Electric Vehicles. In *2018 21st International Conference on Electrical Machines and Systems (ICEMS)* (pp. 871-875). IEEE.

Edwards, K.A., Al-Abed, S.H., Hosseini, S. and Brake, N.A., 2019. Properties of a magnetic concrete core transformer for application in wireless power transfer systems. *Construction and Building Materials*, *227*, p.117041.

Li, F., Sun, X., Zhu, X., Chen, Y., Feng, J., 2021. Magnetization Properties of Pavement Materials and Energy Loss Impact on Wireless Power Transfer. *China Journal of Highway and Transport*, *34*(3), p.71.

Gardner, Trevor, "Wireless Power Transfer Roadway Integration" (2017). Master Thesis, Utah State University.

Hsu, J.U.W., Hu, A.P. and Swain, A., 2009. A wireless power pickup based on directional tuning control of magnetic amplifier. *IEEE Transactions on Industrial Electronics*, *56*(7), pp.2771-2781.

Huang, J., Xiang, S., Wang, Y. and Chen, X., 2021. Energy-saving R&D and carbon intensity in China. *Energy Economics*, *98*, p.105240.

Jasim, A., Wang, H., Yesner, G., Safari, A., and Szary, P. Performance analysis of piezoelectric energy harvesting in pavement: laboratory testing and field simulation, *Transportation Research Record*, 2673(3), pp. 115-124

Jonah, O. and Georgakopoulos, S.V., 2012. Wireless power transfer in concrete via strongly coupled magnetic resonance. *IEEE Transactions on Antennas and Propagation*, *61*(3), pp.1378-1384.

Kalwar, K.A., Aamir, M. and Mekhilef, S., 2015. Inductively coupled power transfer (ICPT) for electric vehicle charging–A review. *Renewable and Sustainable Energy Reviews*, *47*, pp.462-475.

Lazzeroni, P., Cirimele, V. and Canova, A., 2020. Economic and environmental sustainability of Dynamic Wireless Power Transfer for electric vehicles supporting reduction of local air pollutant emissions. *Renewable and Sustainable Energy Reviews*, p.110537.

Li, H., Gao, B., Miao, L., Liu, D., Ma, Q., Tian, G., and Woo, W., 2020. Multiphysics structured eddy current and thermography defects diagnostics system in moving mode. *IEEE Transactions on Industrial Informatics*, 17(4), pp.2566-2578.

Liu, K., Fu, C., Wang, H., Wang, F., Xu, P. and Kan, C., 2020. Exploring the energy-saving potential of electromagnetic induction pavement via magnetic concentrating technique. *Energy*, *211*, p.118650.

Lu, M., Junussov, A. and Bagheri, M., 2020. Analysis of resonant coupling coil configurations of EV wireless charging system: a simulation study. *Frontiers in Energy*, *14*(1), pp.152-165.

Mahmud, M.H., Elmahmoud, W., Barzegaran, M.R. and Brake, N., 2017. Efficient wireless power charging of electric vehicle by modifying the magnetic characteristics of the transmitting medium. *IEEE Transactions on Magnetics*, *53*(6), pp.1-5.

Miller, M., and Daga, A., 2015. Elements of wireless power transfer essential to high power charging of heavy duty vehicles. *IEEE Transactions on Transportation Electrification*, *1*(1), pp.26-39.

Moon, S., Kim, B.C., Cho, S.Y., Ahn, C.H. and Moon, G.W., 2014. Analysis and design of a wireless power transfer system with an intermediate coil for high efficiency. *IEEE Transactions on Industrial Electronics*, *61*(11), pp.5861-5870.

Onar, O.C., Chinthavali, M., Campbell, S.L., Seiber, L.E., White, C.P. and Galigekere, V.P., 2018. Modeling, simulation, and experimental verification of a 20-kw series-series wireless power transfer system for a Toyota RAV4 electric vehicle. In *2018 IEEE Transportation Electrification Conference and Expo (ITEC)*, pp. 874-880.

Shang, J., Tan, Z., Zhang, C. and Ju, L., 2013. The transformer equipment selection's update decision technical and economic analysis model. *Energy and Power Engineering*, *5*(4), pp.143-147.

Shin, J., Shin, S., Kim, Y., Ahn, S., Lee, S., Jung, G., Jeon, S.J. and Cho, D.H., 2013. Design and implementation of shaped magnetic-resonance-based wireless power transfer system for

roadway-powered moving electric vehicles. *IEEE Transactions on Industrial electronics*, *61*(3), pp.1179-1192.

Sun, X., Chen, Y., Feng, J. and Li, F., 2020. Research on the magnetization properties of pavement materials and energy loss impact on wireless power transmission. Presented in 99th Transportation Research Board Annual Conference, Washington, D.C.

Tavakoli, R. and Pantic, Z., 2017. Analysis, design, and demonstration of a 25-kW dynamic wireless charging system for roadway electric vehicles. *IEEE Journal of Emerging and Selected Topics in Power Electronics*, *6*(3), pp.1378-1393.

Venugopal, P., Shekhar, A., Visser, E., Scheele, N., Mouli, G.R.C., Bauer, P. and Silvester, S., 2018. Roadway to self-healing highways with integrated wireless electric vehicle charging and sustainable energy harvesting technologies. *Applied Energy*, *212*, pp.1226-1239.

Wang, H., Zhang, Y., Zhang, Y., Feng, S., Lu, G. and Cao, L., 2019. Laboratory and numerical investigation of microwave heating properties of asphalt mixture. *Materials*, *12*(1), p.146.